Nitrilase Hot Paper

How to cite: *Angew. Chem. Int. Ed.* **2021**, *60*, 3679–3684
International Edition: doi.org/10.1002/anie.202012243
German Edition: doi.org/10.1002/ange.202012243

Inverting the Enantiopreference of Nitrilase-Catalyzed Desymmetric Hydrolysis of Prochiral Dinitriles by Reshaping the Binding Pocket with a Mirror-Image Strategy

Shanshan Yu[+], Jinlong Li[+], Peiyuan Yao[+], Jinhui Feng, Yunfeng Cui, Jianjiong Li, Xiangtao Liu, Qiaqing Wu, Jianping Lin,* and Dunming Zhu**

Abstract: *A mirror-image strategy, that is, symmetry analysis of the substrate-binding pocket, was applied to identify two key amino acid residues W170 and V198 that possibly modulate the enantiopreference of a nitrilase from Synechocystis sp. PCC6803 towards 3-isobutyl glutaronitrile (**1a**). Exchange of these two residues resulted in the enantiopreference inversion (S, 90% ee to R, 47% ee). By further reshaping the substrate-binding pocket via routine site-saturation and combinatorial mutagenesis, variant E8 with higher activity and stereoselectivity (99% ee, R) was obtained. The mutant enzyme was applied in the preparation of optically pure (R)-3-isobutyl-4-cyanobutanoic acid ((R)-**2a**) and showed similar stereopreference inversion towards a series of 3-substituted glutaronitriles. This study may offer a general strategy to switch the stereopreference of other nitrilases and other enzymes toward the desymmetric reactions of prochiral substrates with two identical reactive functional groups.*

Introduction

Chiral γ-amino acids are important building blocks used for the synthesis of pharmaceuticals.[1] Among them, the γ-aminobutyric acid derivatives, (*S*)-3-aminomethyl-5-methyl-hexanoic acid and (*R*)-4-amino-3-(4′-chlorophenyl) butyric acid, are effective components of anticonvulsant Pregabalin (Lyrica)[2] and the muscle relaxant and antispastic agent Baclofen (Lioresal)[3] They are also valuable intermediates for synthesizing other related drugs such as arbaclofen placarbil[4] and (*R*)-rolipram.[5] Enzymatic desymmetrization involving lipase,[6] amidase,[7] nitrilase[8] and one-pot cascade reaction including artificial Michaelase[9] has been applied in the synthesis of γ-aminobutyric acid derivative. However, highly stereoselective and efficient enzyme catalysts remain greatly desired for these biotransformations.

The active pharmaceutical ingredients (*S*)-Pregabalin ((*S*)-**4a**) or (*R*)-Baclofen ((*R*)-**4b**) can be prepared from chiral cyanocarboxylic acid (**2a** or **2b**) through two routes dependent on the absolute configuration of **2a** or **2b**: hydration and subsequent Hofmann rearrangement of (*R*)-**2a** or (*R*)-**2b** (Scheme 1, Route 1),[7b] or Curtius rearrangement followed by hydrolysis of (*S*)-**2a** or (*S*)-**2b** (Scheme 1, Route 2).[8a] In terms of reaction conditions and atomic economy, the Hofmann rearrangement route has some advantages,[10] searching for the (*R*)-selective nitrilase was thus pursued.

Nitrilase-catalyzed desymmetric hydrolysis of 3-substituted glutaronitrile is an important method for the preparation of chiral cyanocarboxylic acids. The desymmetric hydrolysis of 3-benzoyloxy glutaronitrile with high enantiomeric excess (>99% *ee*, *S*) was reported by Ohta et al. using *Rhodococcus rhodochrous* IFO 15564 in 1991.[11] Since then, numbers of microorganisms and nitrilases have been applied for the selective hydrolysis of prochiral dinitrile compounds. Wang and co-workers reported desymmetrization of 3-substituted glutaronitriles by *Rhodococcus* sp. AJ270 with low enantiomeric excess,[8b,12] and the *ee* value of (*S*)-**2b** was improved

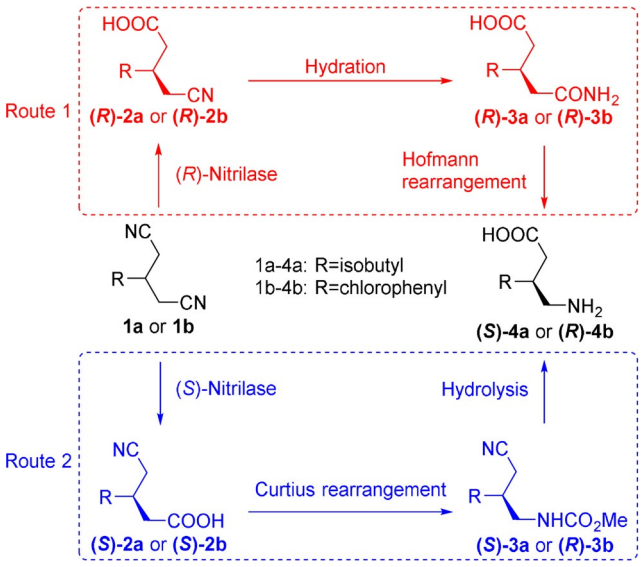

Scheme 1. Synthesis of the active pharmaceutical ingredients (*S*)-Pregabalin ((*S*)-**4a**) and (*R*)-Baclofen ((*R*)-**4b**) via enzymatic desymmetrization.

[*] S. Yu,[+] J. Li,[+] Prof. P. Yao,[+] Prof. J. Feng, Y. Cui, J. Li, X. Liu, Prof. Q. Wu, Prof. J. Lin, Prof. D. Zhu
National Technology Innovation Center of Synthetic Biology
National Engineering Laboratory for Industrial Enzymes and Tianjin Engineering Research Center of Biocatalytic Technology
Tianjin Institute of Industrial Biotechnology
Chinese Academy of Sciences, 32 Xi Qi Dao
Tianjin Airport Economic Area, Tianjin 300308 (P. R. China)
E-mail: wu_qq@tib.cas.cn
lin_jp@tib.cas.cn
zhu_dm@tib.cas.cn

[+] These authors contributed equally to this work.

Supporting information and the ORCID identification number(s) for the author(s) of this article can be found under: https://doi.org/10.1002/anie.202012243.

from 26% to 63% by adding acetone.[13] By screening a large number of nitrilases from various environmental samples, the scientists at Diversa (Verenium) identified numerous nitrilases for the desymmetric hydrolysis of 3-hydroxyglutaronitrile, providing (*S*)-4-cyano-3-hydroxybutyric acid with 98% *ee* or (*R*)-4-cyano-3-hydroxybutyric acid with 95% *ee*.[14] Then, a variant A190H of the most effective (*R*)-nitrilase from environmental samples was obtained to catalyze the hydrolysis of 3-hydroxyglutaronitrile to give (*R*)-4-cyano-3-hydroxybutyric acid in 98% *ee* at high substrate concentrations,[15] but generate (*S*)-**2a** and (*S*)-**2b** in 85% *ee* and 67% *ee*, respectively.[8a] Furthermore, we also tested the desymmetrization of various 3-substituted glutaronitriles using other nitrilases.[8a,16] Among them, (*S*)-configuration products were obtained except AtNIT3, which produced (*R*)-**2b** in 78% *ee* but no activity for **1a**. To the best of our knowledge, the (*R*)-selective nitrilase for desymmetric hydrolysis of 3-alkyl- or aryl substituted glutaronitriles remains rare.

The enantiopreference of an enzyme can be successfully inverted by enzyme engineering,[17] but it is still quite challenging to rapidly achieve it with excellent enantioselectivity and without activity trade-off. Enantiocomplementary enzymes exist in nature to serve as biocatalysts for the synthesis of opposite enantiomers. Although these enzyme pairs are not mirror-image molecules, the active sites of some enantiocomplementary enzymes such as subtilisin Carlsberg and lipase from *Candida rugosa* are identified to be functionally mirror images of one another.[18] By analyzing the crystal structures of vanillyl-alcohol oxidase (VAO) and its enantiocomplementary enzyme *p*-cresol methylhydroxylase (PCMH), D170, a critical residue for the hydration of the initially formed *p*-quinone methide intermediate, was relocated to the opposite face of the active site cavity, creating a D170S/T457E for the transformation of 4-ethylphenol into 1-(4′-hydroxyphenyl)ethanol with an inverted stereopreference.[17q] Thus designing a functional mirror image of an enzyme active site should greatly facilitate the creation of its enantiocomplementary counterpart. Recently, the crystal structure of nitrilase (PDB ID: 3WUY) from *Synechocystis* sp. PCC6803 (*Ss*NIT) has been reported.[19] We found that wild-type enzyme *Ss*NIT exhibited high stereoselectivity toward **1a** (90% *ee*, *S*) and **1b** (97% *ee*, *S*),[8a] and its triple mutant (*Ss*NIT-P194A/I201A/F202V) displayed significantly enhanced catalytic activity and stereoselectivity toward **1b** (99% *ee*, *S*) and other 3-substituted glutaronitriles.[16] Herein, the stereoselectivity of *Ss*NIT was inverted from *S* to *R* toward the desymmetrization of 3-substituted glutaronitriles by a "mirror-image" strategy, that is, symmetry analysis of substrate-binding pocket, followed by site-saturation mutagenesis and combinatorial mutagenesis.

Results and Discussion

To invert the enantioselectivity of *Ss*NIT toward **1a**, alanine scanning of the amino acid residues in the substrate-binding pocket, and subsequent semi-saturated and combinatorial mutagenesis were performed, giving a best (*R*)-selective mutant with 50% *ee* (Supporting Information, Section 1.3, Figure S1, Tables S3–S5). The unsatisfactory results promoted us to seek for different mutation strategies.

High-energy intermediate (HEI) state can reflect early stereoselective recognition of enzymes, which can be treated as the proxies for the typically unknown transition state structure for its chemical similarity with the transition state.[20] Hence, we simulated the HEI state of the hydrolysis reaction by restriction covalent docking based on the reaction mechanism of nitrilase and the crystal structure of nitrilase *Ss*NIT (Figure 1A; Supporting Information, Section 1.9).[19,21] Since **1a** is a symmetrical dinitrile, the ligand molecule was rotated by immobilizing the prochiral center to exchange the positions of two cyano groups, leading to the HEI state for the formation of (*R*)-**2a** (Figure 1B). Herein, we found that the isobutyl of **1a** was blocked by W170.

As such, a mirror-image strategy was proposed as follows: the substrate is centered on the chiral carbon, and its four substituent groups are numbered A, A′, C, and D (as shown in Figure 1C, A and A′ are two identical cyano groups, C and D are isobutyl and hydrogen atom). We speculated that when we interchanged the positions of A and A′, the other two substituent groups C and D will also exchange their positions, leading to the other enantiomeric product after CN hydrolysis. We thus envisioned that the configuration of product **2a** would be inverted by exchanging the two residues (W170 and V198) which interacted with C and D, respectively. Therefore,

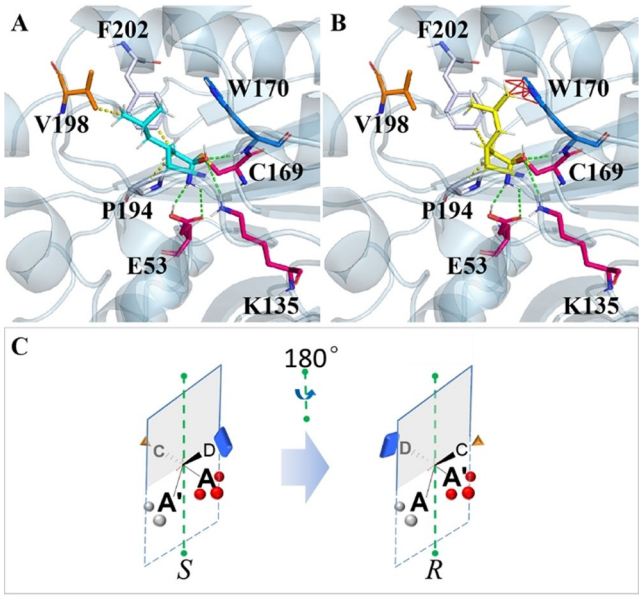

Figure 1. The substrate molecule was restricted covalent docking to the catalytic pocket based on the reaction mechanism. The dotted green line indicates hydrogen bonding interaction, the dotted yellow line indicates hydrophobic interaction, and the solid red line indicates conflict between atoms. A) The HEI state of **1a** (cyan) for formation of (*S*)-**2a**. B) The HEI state of **1a** (yellow) for the formation of (*R*)-**2a** in the catalytic reaction. C) A cartoon of the mirror-image strategy: A, A′, C, and D respectively represent four substituent groups of the prochiral substrate, wherein A and A′ are the two identical CN group, and C, D are two different substituents. The rotation axis (dotted green line) is formed by a tetrahedral structure in accordance with the vertical line of the A-A′ line and the C-D line. Blue blocks, red balls, orange triangles and silver balls represent protein residues.

W170 and V198 were doubly mutated to give W170V/V198W. The resulting mutant enzyme catalyzed the hydrolysis of **1a** to give (*R*)-**2a** with 47% *ee*. Further reducing the bulkiness of residue W170 and adjusting V198 led to mutants W170A/V198W, W170G/V198W (E2) and W170G/V198F, which hydrolyzed **1a** to afford (*R*)-enantiomer in 17% *ee*, 60% *ee* and 82% *ee*, respectively (SI Table S6). Variants W170G/V198W (E2) and W170G/V198F were thus selected for further studies.

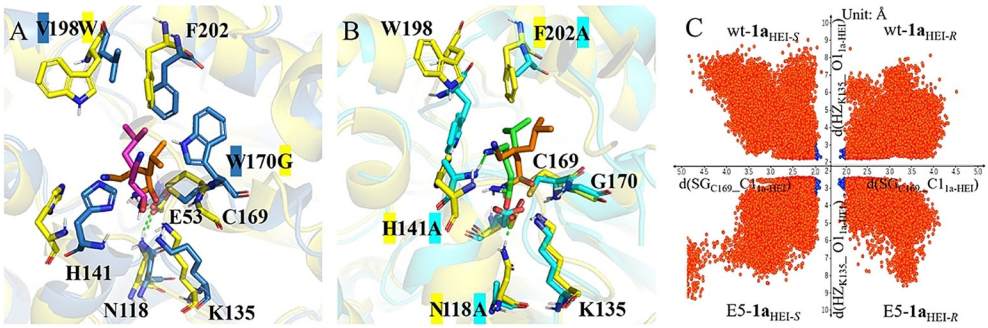

Figure 3. Comparison of catalytic cavity conformations of E2 (yellow) with A) wt *Ss*NIT (blue) and B) E5 (cyan) based on MD analysis. The dotted green line indicates hydrogen bonding interaction. The carbon atoms of substrate in wt-**1a**, E2-**1a** and E5-**1a** are represented by magenta, orange and green, respectively. C) Conformation maps of wt-**1a** and E5-**1a** in dynamical trajectory simulations.

To further improve the stereoselectivity, mutants W170G/V198W (E2) and W170G/V198F were, respectively combined with N118A, H141A and F202A, which showed preference to the formation of (*R*)-enantiomer compared to wild-type enzyme in the alanine scanning studies. Six mutants were constructed and evaluated for the hydrolysis of **1a** (Figure 2; Supporting Information, Table S6). The best mutant W170G/V198W/F202A (E3) led to pronouncedly inverted stereoselectivity in favor of the (*R*)-configuration with 90% *ee*. Other variants included N118A/W170G/V198W (no activity), N118A/W170G/V198F (79% *ee*, *R*), H141A/W170G/V198W (76% *ee*, *R*), H141A/W170G/V198F (34% *ee*, *R*), and W170G/V198F/ F202A (85% *ee*, *R*). The results indicated positive synergistic effects between mutants H141A, F202A and W170G/V198W (E2), and negative effects between variants N118A, H141A and W170G/V198F. Further combinatorial mutants N118A/W170G/V198W/F202A (E4), H141A/W170G/V198W/F202A, and N118A/H141A/W170G/V198W/F202A (E5) were constructed and tested for the hydrolysis of **1a**, and (*R*)-**2a** was obtained in 96%, 93% and 95% *ee*, respectively (Figure 2; Supporting Information, Table S6).

To better understand the evolution of stereoselective inversion, molecular dynamic simulations of wt-**1a**, E2-**1a** and E5-**1a** were performed based on HEI states. The steric hindrance exchange at W170G and V198W made a major contribution to the stereo-preference inversion (Figure 3A). As shown in Figure 3B, residues A141 stabilize the unreacted cyano group by hydrogen bond interactions, while A118 led to the disappearance of hydrogen bonding with E53 enhancing the swing of the catalytic triplet and improved the affinity between mutants and **1a** (Supporting Information, Table S8). Furthermore, the F202A provided more space for isobutyl of **1a**, leading to the orientation of the large steric hindrance group of W198 inclining into binding-pocket and the unreacted cyano group and isobutyl adjusting their orientation. Thus, compared with E2, mutant E5 showed higher stereoselectivity (95% *ee* values) and 8.3- and 23.6-fold improvement in k_{cat} and k_{cat}/K_m, respectively (Supporting Information, Table S8). Furthermore, two distances of sulfydryl of C169 with cyano carbon of **1a**$_{HEI}$ and amino of K135 with hydroxyl of **1a**$_{HEI}$, which support catalysis, in the MD trajectory were calculated as shown in Figure 3C. For wt-**1a**, the proportions of stable HEI-*S* states with both d(SG$_{C169}$-C1$_{1a\text{-}HEI}$) $\leq$2.0 Å and d(HZ$_{K135}$-O1$_{1a\text{-}HEI}$) $\leq$3.5 Å were 0.460%, more than 1.7-fold than that observed in stable HEI-*R* state (0.272%). On the contrary, the stable HEI states (0.540%) in E5-**1a**$_{HEI\text{-}R}$ were 2.6-fold of that observed in E5-**1a**$_{HEI\text{-}S}$ (0.208%). The results indicate that wt-**1a**$_{HEI\text{-}S}$ and E5-**1a**$_{HEI\text{-}R}$ are favorable in the formation of HEI states to give corresponding (*S*)- and (*R*)-**2a**, respectively.

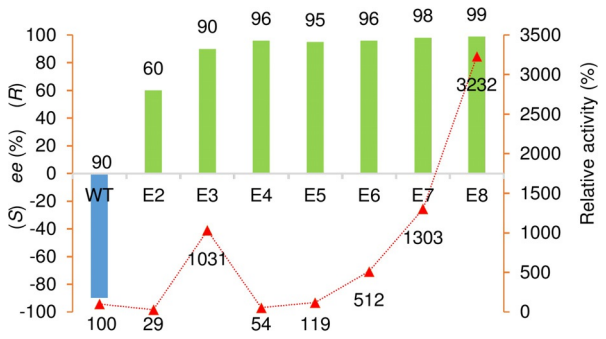

Figure 2. Activity and enantioselectivity of mutants toward the hydrolysis of **1a**. Blue and green bars represent *ee* values with (*S*)- or (*R*)-enantiomer, respectively and red triangle means relative activity. The relative activity of wild-type defined as 100%. The detailed results are presented in the Supporting Information, Tables S6 and S7.

To further improve the activity and stereoselectivity of variant E5 towards **1a**, 14 amino acid residues (Y59, F64, T137, P138, T139, Y140, E142, W146, A168, E171, H172, Y173, F193, P194) located within a distance of 6 Å of **1a** in the docking structure of E5-**1a** (Supporting Information, Figure S2) were selected for site-saturation mutagenesis. Screening of these libraries using **1a** as a substrate by phenol hypochlorite colorimetry method,[22] followed by measuring the *ee* value and the amount of by-product with GC analysis, resulted in three beneficial mutants E5-T137C (E6, 4.3-fold more active relative to E5, 96% *ee*, *R*), E5-A168E (3.23-fold relative to E5, 95% *ee*, *R*) and E5-F193W (2.93-fold relative to E5, 98% *ee*, *R*). Subsequent combinatorial mutagenesis of these beneficial mutants resulted in E5-T137C/A168E (9.7-fold relative to E5, 97% *ee*, *R*), E5-T137C/F193W (E7, 11-

fold relative to E5, 98% *ee*, R) and mutant E5-T137C/A168E/F193W (E8) which exhibited 27.2-fold activity improvement relative to E5 and generated (*R*)-**2a** in 99% *ee* (Figure 2; Supporting Information, Table S7). It is worth noting that variant E8 not only improved the activity and stereoselectivity, but also reduced by-product 3-(cyanomethyl)-5-methylhexanamide (**5a**) to only 0.9% yield.

The k_{cat} and k_{cat}/K_m of mutant E8 were 55.22 min^{-1} and 9.34 $min^{-1}mM^{-1}$ respectively, which exhibited a 23- and 13-fold improvement compared to E5 (Supporting Information, Table S8). The excellent stereoselectivity and activity of E8 could be attributed to a synergistic effect of the three residues. To shed light on the enhanced catalytic activity of E8, the binding modes of E8-**1a** and E5-**1a** were simulated by molecular dynamics, and the HEI state binding energy[23] of E8-**1a** and E5-**1a** was −43.81 kcal mol^{-1} and −39.94 kcal mol^{-1}, respectively. It is notable that the computed binding energy of E8-**1a** is approximately 3.87 kcal mol^{-1} smaller than that of E5-**1a**. Through further binding energy analysis, we found that the binding energy of catalytic triplet with **1a** in mutant E8 was approximately 4.5 kcal mol^{-1} smaller than that of E5-**1a**, implying that mutation of residues T137, A168 and F193 in mutant E8 play a significant role in the difference of binding energy (Supporting Information, Table S9). Additionally, Q192 could form a hydrogen bond with C169 to stabilize catalytic triplet during MD simulation (Supporting Information, Figure S3), but the respective probabilities to form the hydrogen bond in mutant E8 (74.3%) and E5 (22.7%) were dramatically different. Variation in amide **5a** formation was studied by MD sampling of the wt *Ss*NIT and three mutants. The results showed that NH_2 group in the tetrahedral intermediate for the mutant was more easily protonated and resulted in less amide **5a** formation, being consistent with the studies by Jiang et al.[24] (Supporting Information, Table S10).

Specific activity and enantioselectivity of wt *Ss*NIT, and mutants E2, E5 and E8 toward sixteen 3-substituted glutaronitriles were determined. The activity and enantioselectivity were both greatly affected by the amino acid residues in the substrate-binding pocket and the 3-substitutient of glutaronitriles. As shown in Table 1, the variants exhibited similar effects on enantiopreference inversion towards all the tested substrates although they had lower stereoselectivity towards 3-aryl substituted glutaronitriles. Compared to wt *Ss*NIT, variant E8 showed substrate preference to aliphatic dinitrile substrates since E8 exhibited high activity and (*R*)-stereoselectivity toward **1c**–**1f**. The HEI docking study of 3-(4-(trifluoromethyl)phenyl) glutaronitrile (**1p**) showed that for mutant E8, the aromatic ring of (*R*)-configuration interacts with W198, while that of (*S*)-configuration has interaction with Y140 and Y173 (Supporting Information, Figure S4), thus possibly leading to low enantioselectivity. This is reasonable because the substrate-binding pocket was reshaped using **1a** as the model substrate. Therefore, reshaping the substrate-binding pocket to its mirror image to some extent could switch the enzyme stereopreference for a range of similar substrates.

Table 1: Activity and enantioselectivity of wt *Ss*NIT and its variants in the asymmetric hydrolysis of various 3-substitued glutaronitriles **1a**–**1p**.

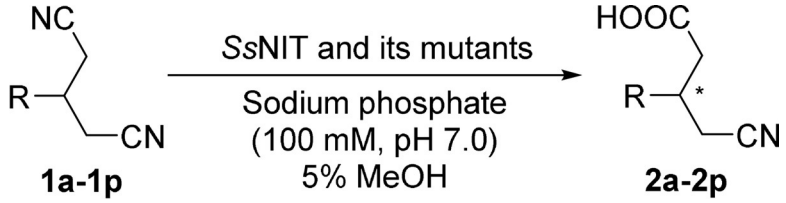

Entry	Substrate	R	Specific activity[a] [mU mg^{-1}] and *ee*[b] [%]							
			WT		E2		E5		E8	
1	**1a**	$((CH_3)_2CHCH_2)$	22	91^S	2	60^R	15	95^R	457	99^R
2	**1b**	$(4\text{-}Cl\text{-}C_6H_4)$	210	97^S	3	48^R	15	16^R	63	23^R
3	**1c**	$(CH_3CH_2CH_2)$	103	95^S	8	28^R	28	77^R	310	91^R
4	**1d**	$(CH_3CH_2CH_2CH_2)$	141	96^S	4	51^R	63	93^R	682	97^R
5	**1e**	$(CH_3CH_2CH_2CH_2CH_2)$	106	96^S	3	80^R	109	99^R	565	99^R
6	**1f**	$((CH_2)_5CH)$	16	98^S	10	29^R	41	99^R	278	99^R
7	**1g**	(C_6H_5)	457	96^S	6	52^R	38	64^R	122	50^R
8	**1h**	$(4\text{-}CH_3\text{-}C_6H_4)$	208	98^S	5	38^R	20	8^R	124	29^R
9	**1i**	$(4\text{-}(CH_3)_2CH\text{-}C_6H_4)$	10	95^S	0	ND[c]	4	91^R	45	70^R
10	**1j**	$(4\text{-}F\text{-}C_6H_4)$	443	99^S	3	54^R	13	49^R	79	34^R
11	**1k**	$(4\text{-}Br\text{-}C_6H_4)$	137	97^S	2	47^R	10	12^R	46	11^R
12	**1l**	$(2\text{-}Cl\text{-}C_6H_4)$	142	74^S	10	35^R	167	49^R	205	38^R
13	**1m**	$(3\text{-}Cl\text{-}C_6H_4)$	397	93^S	4	32^R	60	41^R	169	31^R
14	**1n**	$(4\text{-}CH_3O\text{-}C_6H_4)$	87	98^S	5	71^R	36	88^R	129	76^R
15	**1o**	$(4\text{-}CH_3S\text{-}C_6H_4)$	14	97^S	1	50^R	7	94^R	66	66^R
16	**1p**	$(4\text{-}CF_3\text{-}C_6H_4)$	281	97^S	1	31^R	3	53^R	705	49^R

[a] The activity was determined by the phenol hypochlorite colorimetry reaction. [b] The *ee* value was determined by HPLC on a chiral stationary phase. The absolute configurations of **2a** and **2b** were determined by converting them into the corresponding amino acids and then comparing their retention times with those of the standard samples. The configurations of other products were estimated by comparing their elution sequence in HPLC analysis with those of **2b**. [c] ND = not detected.

The synthesis of (*R*)-**2a** was performed by using whole *E. coli* cells overexpressing variant E8. To investigate the substrate inhibition, various concentrations of **1a** from 100 mM to 500 mM were examined. A complete conversion of 400 mM **1a** was achieved with 99% *ee* (Supporting Information, Figure S6). The synthesis of (*R*)-**2a** was performed at 40 mL scale with substrate loading of 400 mM (60 g L^{-1}). The time course showed that the conversion reached 99% within 24 h and only 0.9% by-product **5a** was detected (Supporting Information, Figure S7). After simple centrifugation and extraction, the desired product (*R*)-**2a** was isolated as yellow oil in > 99% *ee* and 97% yield.

Conclusion

The nitrilase *Ss*NIT was engineered for inverted stereoselectivity from *S* to *R* toward 3-substituted glutaronitriles by directed evolution. A mirror-image strategy was performed to identify key residues responsible for stereo-recognition in the substrate binding pocket, and a simple switch of the two key residues resulted in variant with inverted stereopreference (47% *ee*, *R*). Further reshaping the substrate-binding cavity by site-saturation mutagenesis and combinatorial mutagenesis led to variant E8 with high catalytic efficiency and stereoselectivity (99% *ee*, *R*). MD simulations showed that the mutations changed the probabilities of catalytically active conformations leading to (*S*)- or (*R*)-enantiomer. This is in agreement with the experimental observations. This study provides valuable information for our understanding on how nitrilase controls the enantioselectivity for the desymmetric hydrolysis of various prochiral dinitriles, and the mirror-image strategy may be applicable to other nitrilases and other enzymes for selective desymmetric reactions of prochiral substrates with two identical active functional groups, that are currently tested in our continuing pursue.

Acknowledgements

The work was financially supported by the National Natural Science Foundation of China (Grant No. 21572261), the Youth Innovation Promotion Association of the Chinese Academy of Sciences (Grant No. 2016166), Tianjin Synthetic Biotechnology Innovation Capacity Improvement Project (TSBICIP-KJGG-001) and National Key Research and Development Plan Special Project for "Synthetic biology" (2018YFA0901402).

Conflict of interest

The authors declare no conflict of interest.

Keywords: desymmetric hydrolysis · directed evolution · mirror image · nitrilase · stereopreference inversion

[1] a) R. B. Silverman, R. Andruszkiewicz, S. M. Nanavati, C. P. Taylor, M. G. Vartanian, *J. Med. Chem.* **1991**, *34*, 2295 – 2298; b) J. Farrera-Sinfreu, E. Giralt, S. Castel, F. Albericio, M. Royo, *J. Am. Chem. Soc.* **2005**, *127*, 9459 – 9468; c) M. Ordóñez, C. Cativiela, *Tetrahedron: Asymmetry* **2007**, *18*, 3 – 99; d) M. Ordóñez, C. Cativiela, I. Romero-Estudillo, *Tetrahedron: Asymmetry* **2016**, *27*, 999 – 1055; e) P. Ramesh, D. Suman, K. S. N. Reddy, *Synthesis* **2018**, *50*, 211 – 226; f) S. Wu, R. Snajdrova, J. C. Moore, K. Baldenius, U. T. Bornscheuer, *Angew. Chem. Int. Ed.* **2020**, https://doi.org/10.1002/anie.202006648; *Angew. Chem.* **2020**, https://doi.org/10.1002/ange.202006648; g) B. Hauer, *ACS Catal.* **2020**, *10*, 8418 – 8427.

[2] a) J. E. Frampton, *CNS Drugs* **2014**, *28*, 835 – 854; b) R. Patel, A. H. Dickenson, *Pharmacol. Res. Perspect.* **2016**, *4*, e00205.

[3] a) P. Hudgson, D. Weightman, *Br. Med. J.* **1971**, *4*, 15 – 17; b) N. G. Bowery, D. R. Hill, A. L. Hudson, A. Doble, D. N. Middlemiss, J. Shaw, M. Turnbull, *Nature* **1980**, *283*, 92 – 94.

[4] a) A. Mann, T. Boulanger, B. Brandau, F. Durant, G. Evrard, M. Heaulme, E. Desaulles, C.-G. Wermuth, *J. Med. Chem.* **1991**, *34*, 1307 – 1313; b) R. Lal, J. Sukbuntherng, E. H. L. Tai, S. Upadhyay, F. Yao, M. S. Warren, W. Luo, L. Bu, S. Nguyen, J. Zamora, G. Peng, T. Dias, Y. Bao, M. Ludwikow, T. Phan, R. A. Scheuerman, H. Yan, M. Gao, Q. Q. Wu, T. Annamalai, S. P. Raillard, K. Koller, M. A. Gallop, K. C. Cundy, *J. Pharmacol. Exp. Ther.* **2009**, *330*, 911 – 921.

[5] G.-S. Lee, N. Subramanian, A. I. Kim, I. Aksentijevich, R. Goldbach-Mansky, D. B. Sacks, R. N. Germain, D. L. Kastner, J. J. Chae, *Nature* **2012**, *492*, 123 – 127.

[6] a) C. A. Martinez, S. Hu, Y. Dumond, J. Tao, P. Kelleher, L. Tully, *Org. Process Res. Dev.* **2008**, *12*, 392 – 398; b) J.-H. Jung, D.-H. Yoon, P. Kang, W. K. Lee, H. Euma, H.-J. Ha, *Org. Biomol. Chem.* **2013**, *11*, 3635 – 3641; c) R. Zheng, T. Wang, D. Fu, A. Li, X. Li, Y. Zheng, *Appl. Microbiol. Biotechnol.* **2013**, *97*, 4839 – 4847.

[7] a) L. Zhang, D. Wang, L. Zhao, M. Wang, *J. Org. Chem.* **2012**, *77*, 5584 – 5591; b) M. Nojiri, K. Uekita, M. Ohnuki, N. Taoka, Y. Yasohara, *J. Appl. Microbiol.* **2013**, *115*, 1127 – 1133.

[8] a) Y. Duan, P. Yao, J. Ren, C. Han, Q. Li, J. Yuan, J. Feng, Q. Wu, D. Zhu, *Sci. China Chem.* **2014**, *57*, 1164 – 1171; b) M. Wang, *Acc. Chem. Res.* **2015**, *48*, 602 – 611.

[9] L. Biewenga, T. Saravanan, A. Kunzendorf, J. Y. van der Meer, T. Pijning, P. G. Tepper, R. van Merker, S. J. Charnock, A. W. H. Thunnissen, G. J. Poelarends, *ACS Catal.* **2019**, *9*, 1503 – 1513.

[10] M. S. Hoekstra, D. M. Sobieray, M. A. Schwindt, T. A. Mulhern, T. M. Grote, B. K. Huckabee, V. S. Hendrickson, L. C. Franklin, E. J. Granger, G. L. Karrick, *Org. Process Res. Dev.* **1997**, *1*, 26 – 38.

[11] H. Kakeya, N. Sakai, A. Sano, M. Yokoyama, H. T. Sugai, H. Ohta, *Chem. Lett.* **1991**, *20*, 1823 – 1824.

[12] M. Wang, C. Liu, J. Li, O. Meth-Cohn, *Tetrahedron Lett.* **2000**, *41*, 8549 – 8552.

[13] M. Wang, C. Liu, J. Li, *Tetrahedron: Asymmetry* **2002**, *12*, 3367 – 3373.

[14] a) G. DeSantis, Z. Zhu, W. A. Greenberg, K. Wong, J. Chaplin, S. R. Hanson, B. Farwell, L. W. Nicholson, C. L. Rand, D. P. Weiner, D. E. Robertson, M. J. Burk, *J. Am. Chem. Soc.* **2002**, *124*, 9024 – 9025; b) D. E. Robertson, J. A. Chaplin, G. DeSantis, M. Podar, M. Madden, E. Chi, T. Richardson, A. Milan, M. Miller, D. P. Weiner, K. Wong, J. McQuaid, B. Farwell, L. A. Preston, X. Q. Tan, M. A. Snead, M. Keller, E. Mathur, P. L. Kretz, M. J. Burk, J. M. Short, *Appl. Environ. Microbiol.* **2004**, *70*, 2429 – 2436.

[15] G. DeSantis, K. Wong, B. Farwell, K. Chatman, Z. Zhu, G. Tomlinson, H. Huang, X. Tan, L. Bibbs, P. Chen, K. Kretz, M. J. Burk, *J. Am. Chem. Soc.* **2003**, *125*, 11476 – 11477.

[16] S. Yu, P. Yao, J. Li, J. Feng, Q. Wu, D. Zhu, *Catal. Sci. Technol.* **2019**, *9*, 1504 – 1510.

[17] For changing the entrance tunnel, see: a) A. Shehzad, S. Panneerselvam, M. Linow, M. Bocola, D. Roccatano, J. Mueller-Dieckmann, M. Wilmanns, U. Schwaneberg, *Chem. Commun.* **2013**, *49*, 4694 – 4696; b) H. Ma, X. Yang, Z. Lu, N. Liu, Y. Chen, *PLoS One* **2014**, *9*, e103792; c) J. Zhou, Y. Wang, G. Xu, L. Wu, R. Han, U. Schwaneberg, Y. Rao, Y. L. Zhao, J. Zhou, Y. Ni, *J. Am. Chem. Soc.* **2018**, *140*, 12645 – 12654; For changing substrate binding site, see: d) Y. Ensari, G. V. Dhoke, M. D. Davari, M. Bocola, A. J. Ruff, U. Schwaneberg, *Chem. Eur. J.* **2017**, *23*, 12636 – 12645; e) L. Skalden, C. Peters, J. Dickerhoff, A. Nobili, H. J. Joosten, K. Weisz, M. Hohne, U. T. Bornscheuer, *ChemBioChem* **2015**, *16*, 1041 – 1045; f) X. Chen, H. Zhang, M. A. Maria-Solano, W. Liu, J. Li, J. Feng, X. Liu, S. Osuna, R.-T. Guo, Q. Wu, D. Zhu, Y. Ma, *Nat. Catal.* **2019**, *2*, 931; g) D. Zhang, X. Chen, J. Chi, J. Feng, Q. Wu, D. Zhu, *ACS Catal.* **2015**, *5*, 2452 – 2457; h) D. Zhu, Y. Yang, S. Majkowicz, T. H.-Y. Pan, K. Kantardjieff, L. Hua, *Org. Lett.* **2008**, *10*, 525 – 528; i) E. Eger, A. Simon, M. Sharma, S. Yang, W. B. Breukelaar, G. Grogan, K. N. Houk, W. Kroutil, *J. Am. Chem. Soc.* **2020**, *142*, 792 – 800; j) F. Qin, B. Qin, W. Zhang, Y. Liu, X. Su, T. Zhu, J. Ouyang, J. Guo, Y. Li, F. Zhang, J. Tang, X. Jia, S. You, *ACS Catal.* **2018**, *8*, 6012 – 6020; k) P. Yao, P. Cong, R. Gong, J. Li, G. Li, J. Ren, J. Feng, J. Lin, P. C. K. Lau, Q. Wu, D. Zhu, *ACS Catal.* **2018**, *8*, 1648 – 1652; l) X. Ren, N. Liu, A. L. Chandgude, R. Fasan, *Angew. Chem. Int. Ed.* **2020**, https://doi.org/10.1002/anie.202007953; *Angew. Chem.* **2020**, https://doi.org/10.1002/ange.202007953; m) Z. T. Sun, R. Lonsdale, L. Wu, G. Y. Li, A. T. Li, J. B. Wang, J. H. Zhou, M. T. Reetz, *ACS Catal.* **2016**, *6*, 1590 – 1597; n) A. T. Li, A. Ilie, Z. T. Sun, R. Lonsdale, J. H. Xu, M. T. Reetz, *Angew. Chem. Int. Ed.* **2016**, *55*, 12026 – 12029; *Angew. Chem.* **2016**, *128*, 12205 – 12208; For moving key catalytic residue, see: o) Y. Terao, Y. Ijima, K. Miyamoto, H. Ohta, *J. Mol. Catal. B* **2007**, *45*, 15 – 20; p) Y. Ijima, K. Matoishi, Y. Terao, N. Doi, H. Yanagawa, H. Ohta, *Chem. Commun.* **2005**, 877 – 879; q) R. H. H. van Den Heuvel, M. W. Fraaije, M. Ferrer, A. Mattevi, W. J. van Berkel, *Proc. Natl. Acad. Sci. USA* **2000**, *97*, 9455 – 9460.

[18] a) P. F. Mugford, U. G. Wagner, Y. Jiang, K. Faber, R. J. Kazlauskas, *Angew. Chem. Int. Ed.* **2008**, *47*, 8782 – 8793; *Angew. Chem.* **2008**, *120*, 8912 – 8923; b) P. A. Fitzpatrick, A. M. Klibanov, *J. Am. Chem. Soc.* **1991**, *113*, 3166 – 3171; c) D. L. Ollis, E. Cheah, M. Cygler, B. Dijkstra, F. Frolow, S. M. Franken, M. Harel, S. J. Remington, I. Silman, J. Schrag, *Protein Eng.* **1992**, *5*, 197 – 211; d) R. J. Kazlauskas, A. N. E. Weissfloch, *J. Mol. Catal. B* **1997**, *3*, 65 – 72; e) R. J. K. C. K. Savile, *J. Am. Chem. Soc.* **2005**, *127*, 12228 – 12229; f) Q. Wu, P. Soni, M. T. Reetz, *J. Am. Chem. Soc.* **2013**, *135*, 1872 – 1881; g) S. Bartsch, R. Kourist, U. T. Bornscheuer, *Angew. Chem. Int. Ed.* **2008**, *47*, 1508 – 1511; *Angew. Chem.* **2008**, *120*, 1531 – 1534; h) S. Kim, Y. K. Choi, J. Hong, J. Park, M.-J. Kim, *Tetrahedron Lett.* **2013**, *54*, 1185 – 1188.

[19] L. Zhang, B. Yin, C. Wang, S. Jiang, H. Wang, Y. A. Yuan, D. Wei, *J. Struct. Biol.* **2014**, *188*, 93 – 101.

[20] a) D. N. Bolon, S. L. Mayo, *Proc. Natl. Acad. Sci. USA* **2001**, *98*, 14274 – 14279; b) J. C. Hermann, E. Ghanem, Y. Li, F. M. Raushel, J. J. Irwin, B. K. Shoichet, *J. Am. Chem. Soc.* **2006**, *128*, 15882 – 15891; c) J. C. Hermann, R. Marti-Arbona, A. A. Fedorov, E. Fedorov, S. C. Almo, B. K. Shoichet, F. M. Raushel, *Nature* **2007**, *448*, 775 – 779; d) V. Nanda, R. L. Koder, *Nat. Chem.* **2010**, *2*, 15 – 24; e) M. J. Grisewood, N. P. Gifford, R. J. Pantazes, Y. Li, P. C. Cirino, M. J. Janik, C. D. Maranas, *PLoS One* **2013**, *8*, e75358; f) N. London, J. D. Farelli, S. D. Brown, C. Liu, H. Huang, M. Korczynska, N. F. Al-Obaidi, P. C. Babbitt, S. C. Almo, K. N. Allen, B. K. Shoichet, *Biochemistry* **2015**, *54*, 528 – 537.

[21] B. C. M. Fernandes, C. Mateo, C. Kiziak, A. Chmura, J. Wacker, F. v. Rantwijk, A. Stolz, R. A. Sheldon, *Adv. Synth. Catal.* **2006**, *348*, 2597 – 2603.

[22] a) M. W. Weatherburn, *Anal. Chem.* **1967**, *39*, 971 – 974; b) T. T. Ngo, A. P. H. Phan, C. F. Yam, M. Lenhoff, *Anal. Chem.* **1982**, *54*, 46 – 49; c) Y. Xue, Y. Yang, S. Lv, Z. Liu, Y. Zheng, *Appl. Microbiol. Biotechnol.* **2016**, *100*, 3421 – 3432.

[23] B. R. Miller III, T. D. McGee Jr., J. M. Swails, N. Homeyer, H. Gohlke, A. E. Roitberg, *J. Chem. Theory Comput.* **2012**, *8*, 3314 – 3321.

[24] S. Jiang, L. Zhang, Z. Yao, B. Gao, H. Wang, X. Mao, D. Wei, *Catal. Sci. Technol.* **2017**, *7*, 1122 – 1128.

Manuscript received: September 8, 2020
Revised manuscript received: October 19, 2020
Version of record online: December 14, 2020

